

Article

Icosahedral Polyhedra from D_6 Lattice and Danzer's *ABCK* Tiling

Abeer Al-Siyabi ¹, Nazife Ozdes Koca ^{1,*} and Mehmet Koca ^{2,†}

¹ Department of Physics, College of Science, Sultan Qaboos University, P.O. Box 36, Al-Khoud, Muscat 123, Oman; s21168@student.squ.edu.om

² Department of Physics, Cukurova University, Adana 1380, Turkey; mehmetkocaphysics@gmail.com

* Correspondence: nazife@squ.edu.om

† Retired.

Received: 10 November 2020; Accepted: 26 November 2020; Published: 30 November 2020



Abstract: It is well known that the point group of the root lattice D_6 admits the icosahedral group as a maximal subgroup. The generators of the icosahedral group H_3 , its roots, and weights are determined in terms of those of D_6 . Platonic and Archimedean solids possessing icosahedral symmetry have been obtained by projections of the sets of lattice vectors of D_6 determined by a pair of integers (m_1, m_2) in most cases, either both even or both odd. Vertices of the Danzer's *ABCK* tetrahedra are determined as the fundamental weights of H_3 , and it is shown that the inflation of the tiles can be obtained as projections of the lattice vectors characterized by the pair of integers, which are linear combinations of the integers (m_1, m_2) with coefficients from the Fibonacci sequence. Tiling procedure both for the *ABCK* tetrahedral and the $\langle ABCK \rangle$ octahedral tilings in 3D space with icosahedral symmetry H_3 , and those related transformations in 6D space with D_6 symmetry are specified by determining the rotations and translations in 3D and the corresponding group elements in D_6 . The tetrahedron *K* constitutes the fundamental region of the icosahedral group and generates the rhombic triacontahedron upon the group action. Properties of “*K*-polyhedron”, “*B*-polyhedron”, and “*C*-polyhedron” generated by the icosahedral group have been discussed.

Keywords: lattices; Coxeter–Weyl groups; icosahedral group; projections of polytopes; polyhedra; aperiodic tilings; quasicrystals

1. Introduction

Quasicrystallography as an emerging science attracts the interests of many scientists varying from the fields of material science, chemistry, and physics. For a review, see, for instance, the references [1–3]. It is mathematically intriguing, as it requires the aperiodic tiling of the space by some prototiles. There have been several approaches to describe the aperiodicity of the quasicrystallographic space such as the set theoretic techniques, cut-and-project scheme of the higher dimensional lattices, and the intuitive approaches such as the Penrose-like tilings of the space. For a review of these techniques, we propose the reference [4].

There have been two major approaches for the aperiodic tiling of the 3D space with local icosahedral symmetry. One of them is the Socolar–Steinhardt tiles [5] consisting of acute rhombohedron with golden rhombic faces, Bilinski rhombic dodecahedron, rhombic icosahedron, and rhombic triacontahedron. The latter three are constructed with two Ammann tiles of acute and obtuse rhombohedra. Later, it was proved that [6,7] they can be constructed by the Danzer's *ABCK* tetrahedral tiles [8,9], and recently, Hann–Socolar–Steinhardt [10] proposed a model of tiling scheme with decorated Ammann tiles. A detailed account of the Danzer *ABCK* tetrahedral tilings can be found in [11] and in page 231 of the reference [4] where the substitution matrix, its eigenvalues, and the corresponding

eigenvectors are studied. The right and left eigenvectors of the substitution matrix corresponding to the Perron–Frobenius eigenvalue are well known and will not be repeated here.

Ammann rhombohedral and Danzer *ABCK* tetrahedral tilings are intimately related with the projection of six-dimensional cubic lattice and the root and weight lattices of D_6 , the point symmetry group of which is of order $2^5 6!$. See for a review the paper “Modelling of quasicrystals” by Kramer [12] and references therein. Similar work has also been carried out in the reference [13]. Kramer and Andriele [14] have investigated Danzer tiles from the wavelet point of view and their relations with the lattice D_6 .

In what follows, we point out that the icosahedral symmetry requires a subset of the root lattice D_6 characterized by a pair of integers (m_1, m_2) with $m_1 + m_2 = \text{even}$, which are the coefficients of the orthogonal set of vectors $l_i, (i = 1, 2, \dots, 6)$. Our approach is different than the cut and project scheme of lattice D_6 , as will be seen in the sequel. The paper consists of two major parts; the first part deals with the determination of Platonic and Archimedean icosahedral polyhedra by projection of the fundamental weights of the root lattice D_6 into 3D space, and the second part employs the technique to determine the images of the Danzer tiles in D_6 . Inflation of the Danzer tiles are related to a redefinition of the pair of integers (m_1, m_2) by the Fibonacci sequence. Embeddings of basic tiles in the inflated ones require translations and rotations in 3D space, where the corresponding transformations in 6D space can be easily determined by the technique we have introduced. This technique, which restricts the lattice D_6 to its subset, has not been discussed elsewhere.

The paper is organized as follows. In Section 2, we introduce the root lattice D_6 , its icosahedral subgroup, and decomposition of its weights in terms of the weights of the icosahedral group H_3 leading to the Archimedean polyhedra projected from the D_6 lattice. It turns out that the lattice vectors to be projected are determined by a pair of integers (m_1, m_2) . In Section 3, we introduce the *ABCK* tetrahedral Danzer tiles in terms of the fundamental weights of the icosahedral group H_3 . Tiling by inflation with τ^n where $\tau = \frac{1+\sqrt{5}}{2}$ and $n \in \mathbb{Z}$ is studied in H_3 space by prescribing the appropriate rotation and translation operators. The corresponding group elements of D_6 are determined noting that the pair of integers (m_1, m_2) can be expressed as the linear combinations of similar integers with coefficients from Fibonacci sequence. Section 4 is devoted for conclusive remarks.

2. Projection of D_6 Lattice under the Icosahedral Group H_3 and the Archimedean Polyhedra

We will use the Coxeter diagrams of D_6 and H_3 to introduce the basic concepts of the root systems, weights, and the projection technique. A vector of the D_6 lattice can be written as a linear combination of the simple roots with integer coefficients:

$$\lambda = \sum_{i=1}^6 n_i \alpha_i = \sum_{i=1}^6 m_i l_i, \quad \sum_{i=1}^6 m_i = \text{even}, \quad n_i, m_i \in \mathbb{Z}. \quad (1)$$

Here, α_i are the simple roots of D_6 defined in terms of the orthonormal set of vectors as $\alpha_i = l_i - l_{i+1}, i = 1, \dots, 5$ and $\alpha_6 = l_5 + l_6$, and the reflection generators of D_6 act as $r_i : l_i \longleftrightarrow l_{i+1}$ and $r_6 : l_5 \longleftrightarrow -l_6$. The generators of H_3 can be defined [13] as $R_1 = r_1 r_5, R_2 = r_2 r_4$ and $R_3 = r_3 r_6$, where the Coxeter element, for example, can be taken as $R = R_1 R_2 R_3$. The weights of D_6 are given by

$$\begin{aligned} \omega_1 &= l_1, \quad \omega_2 = l_1 + l_2, \quad \omega_3 = l_1 + l_2 + l_3, \quad \omega_4 = l_1 + l_2 + l_3 + l_4, \\ &= \frac{1}{2}(l_1 + l_2 + l_3 + l_4 + l_5 - l_6), \quad \omega_6 = \frac{1}{2}(l_1 + l_2 + l_3 + l_4 + l_5 + l_6). \end{aligned} \quad (2)$$

The Voronoi cell of the root lattice D_6 is the dual polytope of the root polytope of ω_2 [15] and determined as the union of the orbits of the weights ω_1, ω_5 and ω_6 , which correspond to the holes of the root lattice [16]. If the roots and weights of H_3 are defined in two complementary 3D spaces E_{\parallel} and E_{\perp} as $\beta_i(\hat{\beta}_i)$ and $v_i(\hat{v}_i), (i = 1, 2, 3)$, respectively, then they can be expressed in terms of the roots and weights of D_6 as

$$\begin{aligned} \beta_1 &= \frac{1}{\sqrt{2+\tau}}(\alpha_1 + \tau\alpha_5), \quad v_1 = \frac{1}{\sqrt{2+\tau}}(\omega_1 + \tau\omega_5), \\ \beta_2 &= \frac{1}{\sqrt{2+\tau}}(\alpha_2 + \tau\alpha_4), \quad v_2 = \frac{1}{\sqrt{2+\tau}}(\omega_2 + \tau\omega_4), \\ \beta_3 &= \frac{1}{\sqrt{2+\tau}}(\alpha_6 + \tau\alpha_3), \quad v_3 = \frac{1}{\sqrt{2+\tau}}(\omega_6 + \tau\omega_3). \end{aligned} \tag{3}$$

For the complementary 3D space, replace β_i by $\hat{\beta}_i$, v_i by \hat{v}_i in (3), and $\tau = \frac{1+\sqrt{5}}{2}$ by its algebraic conjugate $\sigma = \frac{1-\sqrt{5}}{2} = -\tau^{-1}$. Consequently, Cartan matrix of D_6 (Gram matrix in lattice terminology) and its inverse block diagonalize as

$$\begin{aligned} C &= \begin{bmatrix} 2 & -1 & 0 & 0 & 0 & 0 \\ -1 & 2 & -1 & 0 & 0 & 0 \\ 0 & -1 & 2 & -1 & 0 & 0 \\ 0 & 0 & -1 & 2 & -1 & -1 \\ 0 & 0 & 0 & -1 & 2 & 0 \\ 0 & 0 & 0 & -1 & 0 & 2 \end{bmatrix} \rightarrow \begin{bmatrix} 2 & -1 & 0 & 0 & 0 & 0 \\ -1 & 2 & -\tau & 0 & 0 & 0 \\ 0 & -\tau & 2 & 0 & 0 & 0 \\ 0 & 0 & 0 & 2 & -1 & 0 \\ 0 & 0 & 0 & -1 & 2 & -\sigma \\ 0 & 0 & 0 & 0 & -\sigma & 2 \end{bmatrix} \\ C^{-1} &= \frac{1}{2} \begin{bmatrix} 2 & 2 & 2 & 2 & 1 & 1 \\ 2 & 4 & 4 & 4 & 2 & 2 \\ 2 & 4 & 6 & 6 & 3 & 3 \\ 2 & 4 & 6 & 8 & 4 & 4 \\ 1 & 2 & 3 & 4 & 3 & 2 \\ 1 & 2 & 3 & 4 & 2 & 3 \end{bmatrix} \rightarrow \frac{1}{2} \begin{bmatrix} 2+\tau & 2\tau^2 & \tau^3 & 0 & 0 & 0 \\ 2\tau^2 & 4\tau^2 & 2\tau^3 & 0 & 0 & 0 \\ \tau^3 & 2\tau^3 & 3\tau^2 & 0 & 0 & 0 \\ 0 & 0 & 0 & 2+\sigma & 2\sigma^2 & \sigma^3 \\ 0 & 0 & 0 & 2\sigma^2 & 4\sigma^2 & 2\sigma^3 \\ 0 & 0 & 0 & \sigma^3 & 2\sigma^3 & 3\sigma^2 \end{bmatrix} \end{aligned} \tag{4}$$

Figure 1 shows how one can illustrate the decomposition of the 6D space as the direct sum of two complementary 3D spaces where the corresponding nodes $\alpha_i, (i = 1, 2, \dots, 6)$, $\beta_i, (i = 1, 2, 3)$ represent the corresponding simple roots, and $\hat{\beta}_i$ stands for β_i in the complementary space.

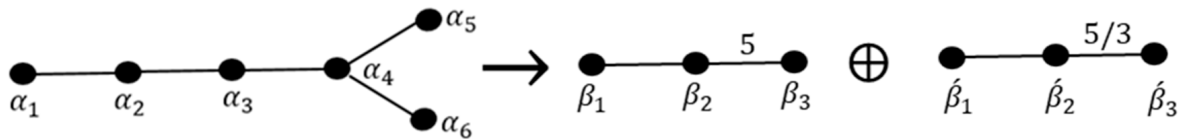


Figure 1. Coxeter-Dynkin diagrams of D_6 and H_3 illustrating the symbolic projection.

For a choice of the simple roots of H_3 as $\beta_1 = (\sqrt{2}, 0, 0)$, $\beta_2 = -\frac{1}{\sqrt{2}}(1, \sigma, \tau)$, $\beta_3 = (0, 0, \sqrt{2})$ and the similar expressions for the roots in the complementary space, we can express the components of the set of vectors $l_i (i = 1, 2, \dots, 6)$ as

$$\begin{bmatrix} l_1 \\ l_2 \\ l_3 \\ l_4 \\ l_5 \\ l_6 \end{bmatrix} = \frac{1}{\sqrt{2(2+\tau)}} \begin{bmatrix} 1 & \tau & 0 & \tau & -1 & 0 \\ -1 & \tau & 0 & -\tau & -1 & 0 \\ 0 & 1 & \tau & 0 & \tau & -1 \\ 0 & 1 & -\tau & 0 & \tau & 1 \\ \tau & 0 & 1 & -1 & 0 & \tau \\ -\tau & 0 & 1 & 1 & 0 & \tau \end{bmatrix} \tag{5}$$

The first three and last three components project the vectors l_i into E_{\parallel} and E_{\perp} spaces, respectively. On the other hand, the weights are represented by the vectors $v_1 = \frac{1}{\sqrt{2}}(1, \tau, 0)$, $v_2 = \sqrt{2}(0, \tau, 0)$, $v_3 = \frac{1}{\sqrt{2}}(0, \tau^2, 1)$. The generators of H_3 in the space E_{\parallel} read

$$R_1 = \begin{bmatrix} -1 & 0 & 0 \\ 0 & 1 & 0 \\ 0 & 0 & 1 \end{bmatrix}, \quad R_2 = \frac{1}{2} \begin{bmatrix} 1 & -\sigma & -\tau \\ -\sigma & \tau & 1 \\ -\tau & 1 & \sigma \end{bmatrix}, \quad R_3 = \begin{bmatrix} 1 & 0 & 0 \\ 0 & 1 & 0 \\ 0 & 0 & -1 \end{bmatrix}, \tag{6}$$

satisfying the generating relations

$$R_1^2 = R_2^2 = R_3^2 = (R_1R_3)^2 = (R_1R_2)^3 = (R_2R_3)^5 = 1 \tag{7}$$

Their representations in the E_{\perp} space follows from (6) by algebraic conjugation. The orbits of the weights v_i under the icosahedral group H_3 can be obtained by applying the group elements on the weight vectors as

$$\begin{aligned} \frac{(v_1)_{H_3}}{\sqrt{2}} &= \frac{1}{2}\{(\pm 1, \pm \tau, 0), (\pm \tau, 0, \pm 1), (0, \pm 1, \pm \tau)\}, \\ \frac{(\tau^{-1}v_2)_{H_3}}{2\sqrt{2}} &= \frac{1}{2}\{(\pm 1, 0, 0), (0, 0, \pm 1), (0, \pm 1, 0), \frac{1}{2}(\pm 1, \pm \sigma, \pm \tau), \frac{1}{2}(\pm \sigma, \pm \tau, \pm 1), \frac{1}{2}(\pm \tau, \pm 1, \pm \sigma)\}, \\ \frac{(\tau^{-1}v_3)_{H_3}}{\sqrt{2}} &= \frac{1}{2}\{(\pm 1, \pm 1, \pm 1), (0, \pm \tau, \pm \sigma), (\pm \tau, \pm \sigma, 0), (\pm \sigma, 0, \pm \tau)\} \end{aligned} \quad (8)$$

where the notation $(v_i)_{H_3}$ is introduced for the set of vectors generated by the action of the icosahedral group on the weight v_i .

The sets of vectors in (8) represent the vertices of an icosahedron, an icosidodecahedron, and a dodecahedron, respectively, in the E_{\parallel} space. The weights v_1 , v_2 , and v_3 also denote the five-fold, two-fold, and three-fold symmetry axes of the icosahedral group. The union of the orbits of $\frac{(v_1)_{H_3}}{\sqrt{2}}$ and $\frac{(\tau^{-1}v_3)_{H_3}}{\sqrt{2}}$ constitute the vertices of a rhombic triacontahedron.

It is obvious that the Coxeter group D_6 is symmetric under the algebraic conjugation, and this is more apparent in the characteristic equation of the Coxeter element of D_6 given by

$$(\lambda^3 + \sigma\lambda^2 + \sigma\lambda + 1)(\lambda^3 + \tau\lambda^2 + \tau\lambda + 1) = 0, \quad (9)$$

whose eigenvalues lead to the Coxeter exponents of D_6 . The first bracket is the characteristic polynomial of the Coxeter element of the matrices in (6) describing it in the E_{\parallel} space, and the second bracket describes it in the E_{\perp} space [17].

Therefore, projection of D_6 into either space is the violation of the algebraic conjugation. It would be interesting to discuss the projections of the fundamental polytopes of D_6 into 3D space possessing the icosahedral symmetry. It is beyond the scope of the present paper; however, we may discuss a few interesting cases.

The orbit generated by the weight ω_1 is a polytope with 12 vertices called cross polytope and represents an icosahedron when projected into either space. The orbit of weight ω_2 constitutes the “root polytope” of D_6 with 60 vertices, which project into 3D space as two icosidodecahedra with 30 vertices each, the ratio of radii of the circumspheres is τ . The dual of the root polytope is the union of the three polytopes generated by ω_1 , ω_5 and ω_6 , which constitute the Voronoi cell of the lattice D_6 , as mentioned earlier and projects into an icosahedron and two rhombic triacontahedra. Actually, they consist of three icosahedra with the ratio of radii $1, \tau, \tau^2$ and two dodecahedra with the radii in proportion to τ . The orbit generated by the weight vector ω_3 is a polytope with 160 vertices and constitutes the Voronoi cell of the weight lattice D_6^* . It projects into two dodecahedra and two polyhedra with 60 vertices each. Voronoi cells can be used as windows for the cut and projects scheme; however, we prefer the direct projection of the root lattice as described in what follows.

A general root vector can be decomposed in terms of the weights $v_i(\hat{v}_i)$ as

$$\begin{aligned} m_1l_1 + m_2l_2 + m_3l_3 + m_4l_4 + m_5l_5 + m_6l_6 \\ = \frac{1}{\sqrt{2+\tau}}[(m_1 - m_2 + \tau m_5 - \tau m_6)v_1 + (m_2 - m_3 + \tau m_4 - \tau m_5)v_2 \\ + (m_5 + m_6 + \tau m_3 - \tau m_4)v_3] + (v_i \rightarrow \hat{v}_i, \tau \rightarrow \sigma). \end{aligned} \quad (10)$$

Projection of an arbitrary vector of D_6 into the space E_{\parallel} , or more thoroughly, onto a particular weight vector, for example, onto the weight v_1 is given by

$$[m_1l_1 + m_2(l_2 + l_3 + l_4 + l_5 - l_6)]_{\parallel} \equiv [(m_1 - m_2)\omega_1 + 2m_2\omega_5]_{\parallel} = c\left(\frac{v_1}{\sqrt{2}}\right) \quad (11)$$

And represents an icosahedron where $c \equiv c(m_1, m_2) = \sqrt{\frac{2}{2+\tau}}(m_1 - m_2 + 2m_2\tau)$ is an overall scale factor. The subscript \parallel means the projection into the space E_{\parallel} . The expression in (11) shows that $m_1 + m_2 = \text{even}$, implying that the pair of integers (m_1, m_2) are either both even or both odd. We will see that not only icosahedron but also dodecahedron and the icosahedral Archimedean polyhedra can be obtained by relations similar to (11). The Platonic and Archimedean polyhedra with icosahedral symmetry are listed in Table 1 as projections of D_6 lattice vectors determined by the pair of integers (m_1, m_2) . Table 1 shows that only a certain subset of vectors of D_6 project onto regular icosahedral polyhedra. We will see in the next section that the Danzer tiling also restricts the D_6 lattice in a domain, where the vectors are determined by the pair of integers (m_1, m_2) . These quantities studied here are potentially applicable to many graph indices [18].

Table 1. Platonic and Archimedean icosahedral polyhedra projected from D_6 (vertices are orbits under the icosahedral group).

Vector of the Polyhedron in H_3		Corresponding Vector in D_6
$c \equiv \sqrt{\frac{2}{2+\tau}}(m_1 - m_2 + 2m_2\tau)$		$m_1, m_2 \in \mathbb{Z}$
Icosahedron $c \frac{v_1}{\sqrt{2}} = \frac{c}{2}(1, \tau, 0)$		$m_1l_1 + m_2(l_2 + l_3 + l_4 + l_5 - l_6) = (m_1 - m_2)\omega_1 + 2m_2\omega_5$ $m_1, m_2 \in 2\mathbb{Z} \text{ or } 2\mathbb{Z} + 1$
Dodecahedron $c \frac{v_3}{\sqrt{2}} = \frac{c}{2}(0, \tau^2, 1)$		$\frac{1}{2}[(m_1 + 3m_2)(l_1 + l_2 + l_3) + (m_1 - m_2)(l_4 + l_5 + l_6)] =$ $(m_1 - m_2)\omega_6 + 2m_2\omega_3$ $m_1, m_2 \in 2\mathbb{Z} \text{ or } 2\mathbb{Z} + 1$
Icosidodecahedron $c \frac{v_2}{\sqrt{2}} = c(0, \tau, 0)$		$(m_1 + m_2)(l_1 + l_2) + 2m_2(l_3 + l_4) =$ $(m_1 - m_2)\omega_2 + 2m_2\omega_4$ $m_1, m_2 \in 2\mathbb{Z} \text{ or } 2\mathbb{Z} + 1$
Truncated Icosahedron $c \frac{(v_1+v_2)}{\sqrt{2}} = \frac{c}{2}(1, 3\tau, 0)$		$(2m_1 + m_2)l_1 + (m_1 + 2m_2)l_2 +$ $m_2(3l_3 + 3l_4 + l_5 - l_6) =$ $(m_1 - m_2)(\omega_1 + \omega_2) + 2m_2(\omega_4 + \omega_5)$ $m_1, m_2 \in 2\mathbb{Z} \text{ or } 2\mathbb{Z} + 1$
Small Rhombicosidodecahedron $c \frac{(v_1+v_3)}{\sqrt{2}} = \frac{c}{2}(1, 2\tau + 1, 1)$		$\frac{1}{2}[(3m_1 + 3m_2)l_1 + (m_1 + 5m_2)(l_2 + l_3)$ $+ (m_1 + m_2)(l_4 + l_5) + (m_1 - 3m_2)l_6]$ $= (m_1 - m_2)(\omega_1 + \omega_6) + 2m_2(\omega_3 + \omega_5)$
Truncated Dodecahedron $c \frac{(v_2+v_3)}{\sqrt{2}} = \frac{c}{2}(0, 3\tau + 1, 1)$		$\frac{1}{2}[(3m_1 + 5m_2)(l_1 + l_2) + (m_1 + 7m_2)l_3 + (m_1 + 3m_2)l_4$ $+ (m_1 - m_2)(l_5 + l_6)]$ $= (m_1 - m_2)(\omega_2 + \omega_6) + 2m_2(\omega_3 + \omega_4)$
Great Rhombicosidodecahedron $c \frac{(v_1+v_2+v_3)}{\sqrt{2}} = \frac{c}{2}(1, 4\tau + 1, 1)$		$\frac{1}{2}[5(m_1 + m_2)l_1 + (3m_1 + 7m_2)l_2 + (m_1 + 9m_2)l_3$ $+ (m_1 + 5m_2)l_4 + (m_1 + m_2)l_5 + (m_1 - 3m_2)l_6]$ $= (m_1 - m_2)(\omega_1 + \omega_2 + \omega_6) + 2m_2(\omega_3 + \omega_4 + \omega_5)$

3. Danzer’s ABCK Tiles and D_6 Lattice

We introduce the $ABCK$ tiles with their coordinates in Figure 2 as well as their images in lattice D_6 . For a fixed pair of integers $(m_1, m_2) \neq (0, 0)$, let us define the image of K by vertices $D_1(m_1, m_2)$, $D_2(m_1, m_2)$, $D_3(m_1, m_2)$, and $D_0(0, 0)$ in lattice D_6 and its projection in 3D space, where $D_0(0, 0)$ represents the origin. They are given as

$$\begin{aligned} D_1(m_1, m_2) &= \frac{cv_1}{\sqrt{2}} = [m_1l_1 + m_2(l_2 + l_3 + l_4 + l_5 - l_6)]_{\parallel} = [(m_1 - m_2)\omega_1 + 2m_2\omega_5]_{\parallel} \\ D_2(m_1, m_2) &= \frac{cv_2}{2\sqrt{2}} = \frac{1}{2}[(m_1 + m_2)(l_1 + l_2) + 2m_2(l_3 + l_4)]_{\parallel} = \frac{1}{2}[(m_1 - m_2)\omega_2 + 2m_2\omega_4]_{\parallel} \\ D_3(m_1, m_2) &= \frac{c\tau^{-1}v_3}{\sqrt{2}} = \frac{1}{2}[(m_1 + m_2)(l_1 + l_2 + l_3) + (-m_1 + 3m_2)(l_4 + l_5 + l_6)]_{\parallel} \\ &= [2m_2\omega_3 + (-m_1 + 3m_2)\omega_6]_{\parallel} \end{aligned} \tag{12}$$

which follows from Table 1 with redefinitions of the pair of integers (m_1, m_2) . With removal of the notation \parallel , they represent the vectors in 6D space. A set of scaled vertices defined by $\hat{D}_i \equiv \frac{D_i(m_1, m_2)}{c}$ are used for the vertices of the Danzer’s tetrahedra in Figure 2.

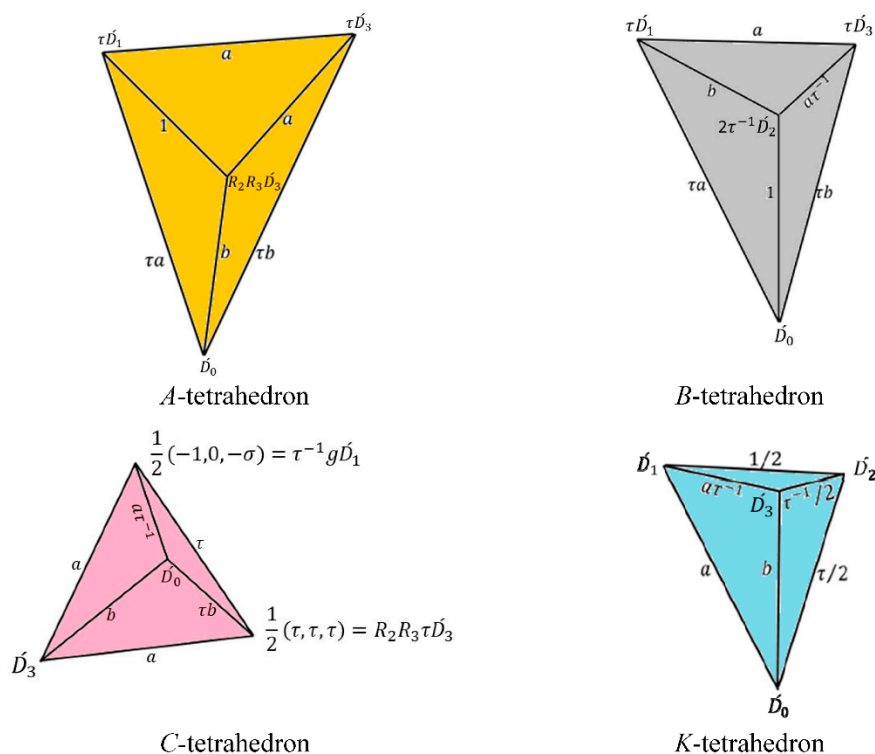


Figure 2. Danzer’s tetrahedra.

It is instructive to give a brief introduction to Danzer’s tetrahedra before we go into details. The edge lengths of ABC tetrahedra are related to the weights of the icosahedral group H_3 whose edge lengths are given by $a = \frac{\sqrt{2+\tau}}{2} = \frac{\|v_1\|}{\sqrt{2}}$, $b = \frac{\sqrt{3}}{2} = \frac{\|\tau^{-1}v_3\|}{\sqrt{2}}$, $1 = \frac{\|\tau^{-1}v_2\|}{\sqrt{2}}$ and their multiples by τ and τ^{-1} , where $a, b, 1$ are the original edge lengths introduced by Danzer. However, the tetrahedron K has edge lengths also involving $\frac{1}{2}$, $\frac{\tau}{2}$, $\frac{\tau^{-1}}{2}$. As we noted in Section 2, the vertices of a rhombic triacontahedron consist of the union of the orbits $\frac{(v_1)_{H_3}}{\sqrt{2}}$ and $\frac{(\tau^{-1}v_3)_{H_3}}{\sqrt{2}}$. One of its cells is a pyramid based on a golden rhombus with vertices

$$\frac{v_1}{\sqrt{2}} = \frac{1}{2}(1, \tau, 0), \frac{\tau^{-1}v_3}{\sqrt{2}} = \frac{1}{2}(0, \tau, -\sigma), R_1 \frac{v_1}{\sqrt{2}} = \frac{1}{2}(-1, \tau, 0), R_3 \frac{\tau^{-1}v_3}{\sqrt{2}} = \frac{1}{2}(0, \tau, \sigma), \tag{13}$$

And the apex is at the origin. The coordinate of the intersection of the diagonals of the rhombus is the vector $\frac{v_2}{2\sqrt{2}} = \frac{1}{2}(0, \tau, 0)$, and its magnitude is the in-radius of the rhombic triacontahedron. Therefore, the weights $\frac{v_1}{\sqrt{2}}, \frac{\tau^{-1}v_3}{\sqrt{2}}, \frac{v_2}{2\sqrt{2}}$ and the origin can be taken as the vertices of the tetrahedron K . As such, it is the fundamental region of the icosahedral group from which the rhombic triacontahedron is generated [19]. The octahedra generated by these tetrahedra denoted by $\langle B \rangle, \langle C \rangle$ and $\langle A \rangle$ comprise four copies of each obtained by a group of order four generated by two commuting generators R_1 and R_3 or their conjugate groups. The octahedron $\langle K \rangle$ consists of $8K$ generated by a group of order eight consisting of three commuting generators R_1, R_3 as mentioned earlier, and the third generator R_0 is an affine reflection [20] with respect to the golden rhombic face induced by the affine Coxeter group \widetilde{D}_6 .

One can dissect the octahedron $\langle K \rangle$ into three non-equivalent pyramids with rhombic bases by cutting along the lines orthogonal to three planes $v_1 - v_2, v_2 - v_3, v_3 - v_1$. One of the pyramids is generated by the tetrahedron K upon the actions of the group generated by the reflections R_1 and R_3 . If we call $R_1K = \acute{K}$ as the mirror image of K the others can be taken as the tetrahedra obtained from K and R_1K by a rotation of 180° around the axis v_2 . A mirror image of $4K = (2K + 2\acute{K})$ with respect to the rhombic plane (corresponding to an affine reflection) complements it up to an octahedron of $8K$, as we mentioned above. In addition to the vertices in (13) the octahedron $8K$ also includes the vertices $(0, 0, 0)$ and $(0, \tau, 0)$. Octahedral tiles are depicted in Figure 3. Dissected pyramids constituting the octahedron $\langle K \rangle$, as depicted in Figure 4, have bases, two of which with bases of golden rhombuses with edge lengths (heights) $\tau^{-1}a(\frac{\tau}{2}), a(\frac{\tau^{-1}}{2})$, and the third is the one with $b(\frac{1}{2})$. The rhombic triacontahedron consists of $60K + 60\acute{K} = 30(2K + 2\acute{K})$, where $(2K + 2\acute{K})$ form a cell of pyramid based on a golden rhombus of edge $\tau^{-1}a$ and height $\frac{\tau}{2}$. Faces of the rhombic triacontahedron are the rhombuses orthogonal to one of 30 vertices of the icosidodecahedron given in (8).

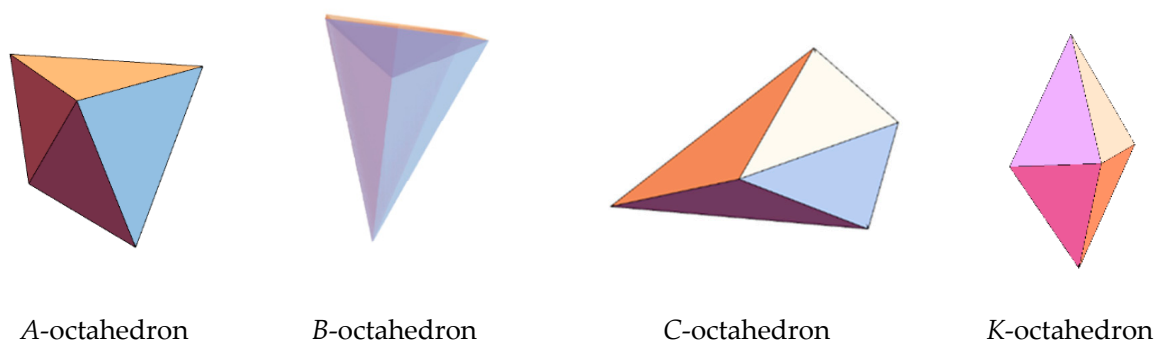


Figure 3. The octahedra generated by the $ABCK$ tetrahedra.

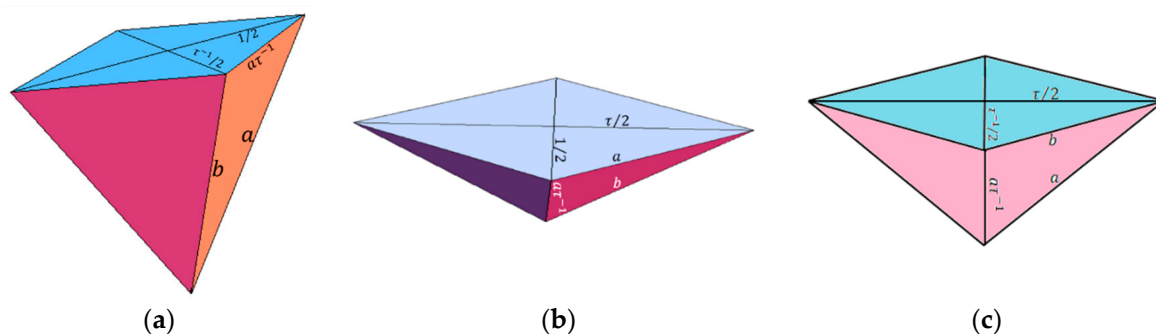


Figure 4. The three pyramids (a–c) composed of $4K$ tetrahedra.

When the $4K$ of Figure 4a is rotated by the icosahedral group, it generates the rhombic triacontahedron as shown in Figure 5.



Figure 5. A view of rhombic triacontahedron.

The octahedron $\langle B \rangle$ is a non-convex polyhedron whose vertices can be taken as $\hat{D}_1, \tau R_1 \hat{D}_1, \tau \hat{D}_3, \tau R_3 \hat{D}_3, 2\tau^{-1} \hat{D}_2$, and the sixth vertex is the origin \hat{D}_0 . It consists of four triangular faces with edges $a, \tau a, \tau b$ and four triangular faces with edges $\tau^{-1} a, a, b$. Full action of the icosahedral group on the tetrahedron B would generate the “ B -polyhedron” consisting of $60B + 60\hat{B}$ where $\hat{B} = R_1 B$ is the mirror image of B . It has 62 vertices (12 like $\frac{(\tau v_1)_{h_3}}{\sqrt{2}}$, 30 like $\frac{(\tau^{-1} v_2)_{h_3}}{\sqrt{2}}$, 20 like $\frac{(v_3)_{h_3}}{\sqrt{2}}$), 180 edges, and 120 faces consisting of faces with triangles of edges with $\tau^{-1} a, a, b$. The face transitive “ B -polyhedron” is depicted in Figure 6 showing three-fold and five-fold axes simultaneously.

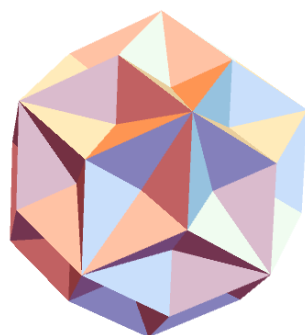


Figure 6. The “ B -polyhedron”.

The octahedron $\langle C \rangle$ is a convex polyhedron, which can be represented by the vertices

$$\frac{1}{2}(\tau, 0, 1), \frac{1}{2}(\tau, \tau, \tau), \frac{1}{2}(1, \tau, 0), \frac{1}{2}(\tau^2, 1, 0), \frac{1}{2}(\tau^2, \tau, 1), (0, 0, 0). \tag{14}$$

This is obtained from that of Figure 2 by a translation and inversion. It consists of four triangular faces with edges $a, b, \tau b$ and four triangular faces with edges $\tau^{-1} a, a$ and b .

The “ C -polyhedron” is a non-convex polyhedron with 62 vertices (12 like $\frac{(v_1)_{h_3}}{\sqrt{2}}$, 30 like $\frac{(v_2)_{h_3}}{\sqrt{2}}$, 20 like $\frac{(v_3)_{h_3}}{\sqrt{2}}$), 180 edges, and 120 faces consisting of only one type of triangular face with edge lengths $\tau^{-1} a, a$ and b as can be seen in Figure 7 (see also the reference [4]). It is also face transitive same as “ B -polyhedron”.

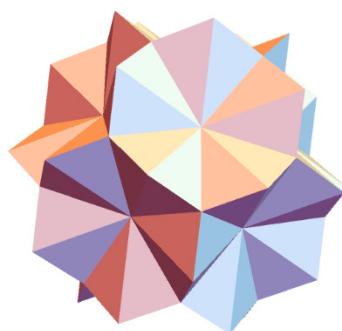


Figure 7. The “ C -polyhedron”.

The octahedron $\langle A \rangle$ is a non-convex polyhedron, which can be represented by the vertices

$$\frac{1}{2}(-\tau, 0, 1), \frac{1}{2}(1, -\tau, 0), \frac{1}{2}(1, 1, 1), \frac{1}{2}(\sigma, 0, -\tau), \frac{1}{2}(\sigma, -\tau, 1), (0, 0, 0), \tag{15}$$

as shown in Figure 3.

Now, we discuss how the tiles are generated by inflation with an inflation factor τ . First of all, let us recall that the projection of subset of the D_6 vectors specified by the pair of integers (m_1, m_2) are some linear combinations of the weights $v_i, (i = 1, 2, 3)$ with an overall factor c . It is easy to find out the vector of D_6 corresponding to the inflated vertex of any $ABCK$ tetrahedron by noting that $c(\tau^n v_i) = c(\acute{m}_1, \acute{m}_2) v_i$. Here, we use $\tau^n = F_{n-1} + F_n \tau$, and we define

$$\acute{m}_1 \equiv m_1 F_{n-1} + \frac{1}{2}(m_1 + 5m_2) F_n, \quad \acute{m}_2 \equiv m_2 F_{n-1} + \frac{1}{2}(m_1 + m_2) F_n, \tag{16}$$

where F_n represents the Fibonacci sequence satisfying

$$F_{n+1} = F_n + F_{n-1}, F_{-n} = (-1)^{n+1} F_n, F_0 = 0, F_1 = 1. \tag{17}$$

It follows from (16) that $\acute{m}_1 + \acute{m}_2 =$ even if $m_1 + m_2 =$ even, otherwise $\acute{m}_1, \acute{m}_2 \in \mathbb{Z}$. This proves that the pair of integers $(\acute{m}_1, \acute{m}_2)$ obtained by inflation of the vertices of the Danzer’s tetrahedra remain in the subset of D_6 lattice. We conclude that the inflated vectors by τ^n in (12) can be obtained by replacing m_1 by \acute{m}_1 and m_2 by \acute{m}_2 . For example, radii of the icosahedra projected by D_6 vectors

$$2\omega_1, 2\omega_5, 2\omega_1 + 2\omega_5, 2\omega_1 + 4\omega_5 \tag{18}$$

are in proportion to $1, \tau, \tau^2$ and τ^3 , respectively. It will not be difficult to obtain the D_6 image of any general vector in the 3D space in the form of $c(\tau^p, \tau^q, \tau^r)$ where $p, q, r \in \mathbb{Z}$. Now we discuss the inflation of each tile one by one.

3.1. Construction of $\tau K = B + K$

The vertices of τK is shown in Figure 8 where the origin coincides with one of the vertices of B as shown in Figure 2 and the other vertices of K and B are depicted. A transformation is needed to translate K to its new position. The face of K opposite to the vertex \acute{D}_2 having a normal vector $\frac{1}{2}(-1, -\sigma, -\tau)$ outward should match with the face of B opposite to the vertex \acute{D}_0 with a normal vector $\frac{1}{2}(\sigma, \tau, -1)$ inward. For this reason, we perform a rotation of K given by

$$g_K = \begin{bmatrix} 0 & -1 & 0 \\ 0 & 0 & -1 \\ 1 & 0 & 0 \end{bmatrix} \tag{19}$$

matching the normal of these two faces. A translation by the vector $\frac{1}{2}(\tau, \tau^2, 0)$ will locate K in its proper place in τK . This is the simplest case where a rotation and a translation would do the work. The corresponding rotation and translation in D_6 can be calculated easily, and the results are illustrated in Table 2.

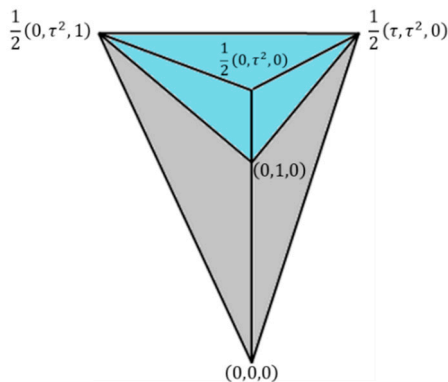


Figure 8. Vertices of τK .

Table 2. Rotation and translation in H_3 and D_6 .

H_3		D_6
g_K	←rotation→	$g_K : (\overline{136})(24\overline{5})$
$t_K = \frac{1}{2}(\tau, \tau^2, 0)$	←translation→	$\frac{1}{2}[(m_1 + 5m_2)l_1 + (m_1 + m_2)(l_2 + l_3 + l_4 + l_5 - l_6)]$

The rotation in D_6 is represented as the permutations of components of the vectors in the l_i basis.

Rhombic triacontahedron generated by τK now consists of a “B-Polyhedron” centered at the origin and 30 pyramids of $4K$ with golden rhombic bases of edge lengths a and heights $\frac{\tau^{-1}}{2}$ occupy the 30 inward gaps of “B-Polyhedron”.

3.2. Construction of $\tau B = C + 4K + B_1 + B_2$

The first step is to rotate B by a matrix

$$g_B = \frac{1}{2} \begin{bmatrix} -\sigma & \tau & -1 \\ -\tau & 1 & -\sigma \\ 1 & -\sigma & \tau \end{bmatrix} \tag{20}$$

and then inflate by τ to obtain the vertices of $\tau g_B B$ as shown in Figure 9.

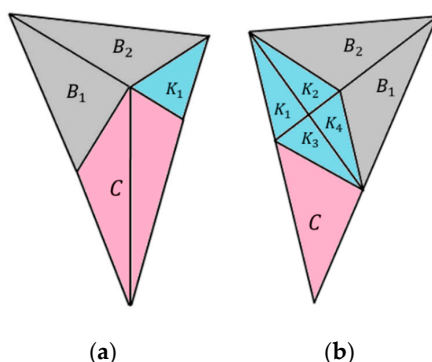


Figure 9. Views from $\tau g_B B$. (a) Top view of $\tau g_B B$; (b) bottom view of $\tau g_B B$.

Representation of $\tau g_B B$ is chosen to coincide the origin with the \hat{D}_0 vertex of tetrahedron C . It is obvious to see that the bottom view illustrates that the $4K$ is the pyramid based on the rhombus with edge length (height), $b(\frac{1}{2})$ as shown in Figure 4c. The $4K$ takes its position in Figure 9 by a rotation followed by a translation given by

$$\text{rotation : } g_{4K} = \frac{1}{2} \begin{bmatrix} 1 & -\sigma & -\tau \\ -\sigma & \tau & 1 \\ -\tau & 1 & \sigma \end{bmatrix}, \text{ translation : } t_{4K} = \frac{1}{2}(\tau, 0, 1). \tag{21}$$

To translate B_1 and B_2 , we follow the rotation and translation sequences as

$$\begin{aligned} \text{rotation : } g_{B_1} &= \frac{1}{2} \begin{bmatrix} \sigma & -\tau & 1 \\ -\tau & 1 & -\sigma \\ -1 & \sigma & -\tau \end{bmatrix}, \text{ translation : } t_B = \frac{1}{2}(\tau^3, 0, \tau^2), \\ \text{rotation : } g_{B_2} &= \frac{1}{2} \begin{bmatrix} -\sigma & -\tau & 1 \\ \tau & 1 & -\sigma \\ 1 & \sigma & -\tau \end{bmatrix}, \text{ translation : } t_B = \frac{1}{2}(\tau^3, 0, \tau^2). \end{aligned} \tag{22}$$

3.3. Construction of $\tau C = K_1 + K_2 + C_1 + C_2 + A$

We inflate by τ the tetrahedron C with vertices shown in Figure 10. Top view of τC where one of the vertices of K_1 is at the origin is depicted in Figure 11. The vertices of the constituting tetrahedra are given as follows:

$$\begin{aligned}
 K_1 &: \left\{ (0,0,0), \frac{1}{2}(1,1,1), \frac{1}{2}(\tau,0,1), \frac{1}{4}(\tau^2, \tau, 1) \right\}; \\
 K_2 &: \left\{ \frac{1}{2}(1,1,1), \frac{1}{2}(\tau,0,1), \frac{1}{4}(\tau^2, \tau, 1), \frac{1}{2}(\tau^2, \tau, 1) \right\}; \\
 C_1 &: \left\{ \frac{1}{2}(1,1,1), \frac{1}{2}(\tau,0,1), \frac{1}{2}(\tau^2, \tau, 1), \frac{1}{2}(\tau^2, \tau^2, \tau^2) \right\}; \\
 C_2 &: \left\{ \frac{1}{2}(\tau,0,1), \frac{1}{2}(\tau^2, \tau, 1), \frac{1}{2}(\tau^2, 0, \tau), \frac{1}{2}(\tau^2, \tau^2, \tau^2) \right\}; \\
 A &: \left\{ \frac{1}{2}(\tau^2, \tau, 1), \frac{1}{2}(\tau^2, 0, \tau), \frac{1}{2}(\tau^2, \tau^2, \tau^2), \frac{1}{2}(\tau^3, \tau^2, \tau) \right\}.
 \end{aligned}
 \tag{23}$$

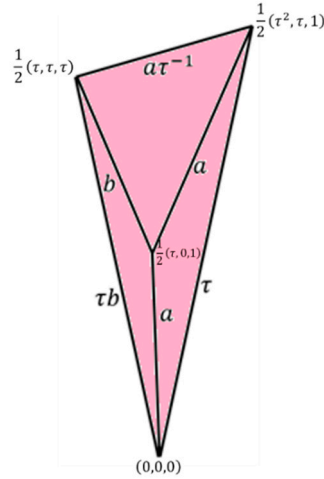


Figure 10. C-tetrahedron obtained from that of Figure 2 by translation and inversion.

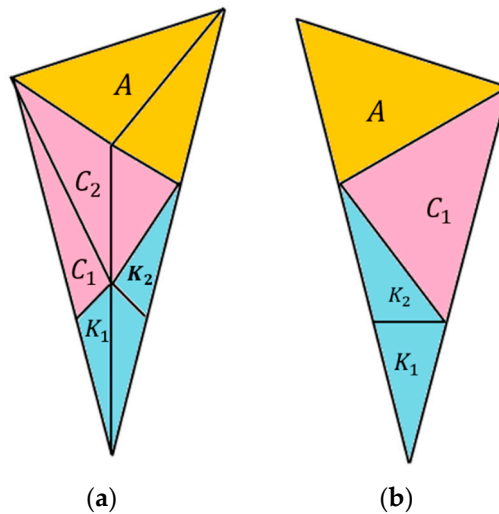


Figure 11. Views from τC . (a) Top view of τC ; (b) bottom view of τC .

The vertices of K_1 can be obtained from K by a rotation $K_1 = g_{K_1}K$, where

$$g_{K_1} = \frac{1}{2} \begin{bmatrix} -\sigma & \tau & -1 \\ -\tau & 1 & -\sigma \\ 1 & -\sigma & \tau \end{bmatrix}, \quad (g_{K_1})^5 = 1.
 \tag{24}$$

The transformation to obtain K_2 is a rotation g_{K_2} followed by a translation of $t_{K_2} = \frac{1}{2}(\tau^2, \tau, 1)$, where

$$g_{K_2} = \frac{1}{2} \begin{bmatrix} -\sigma & -\tau & -1 \\ -\tau & -1 & -\sigma \\ 1 & \sigma & \tau \end{bmatrix}, \quad (g_{K_2})^{10} = 1
 \tag{25}$$

To obtain the coordinates of C_1 and C_2 , first translate C by $-\frac{1}{2}(\tau, \tau, \tau)$ and rotate by g_{C_1} and g_{C_2} , respectively, followed by the translation $t_{C_1} = \frac{1}{2}(\tau^2, \tau^2, \tau^2)$, where

$$g_{C_1} = \frac{1}{2} \begin{bmatrix} \sigma & \tau & 1 \\ \tau & 1 & \sigma \\ 1 & \sigma & \tau \end{bmatrix}, \quad g_{C_2} = \frac{1}{2} \begin{bmatrix} 1 & -\sigma & -\tau \\ -\sigma & \tau & 1 \\ \tau & -1 & -\sigma \end{bmatrix} \quad (26)$$

Similarly, vertices of tetrahedron A are rotated by

$$g_A = \frac{1}{2} \begin{bmatrix} 1 & -\sigma & -\tau \\ -\sigma & \tau & 1 \\ -\tau & 1 & \sigma \end{bmatrix} \quad (27)$$

followed by a translation $t_A = \frac{1}{2}(\tau^2, 0, \tau)$.

3.4. Construction of $\tau A = 3B + 2C + 6K$

It can also be written as $\tau A = C + K_1 + K_2 + B + \tau B$, where τB is already studied. A top view of τA is depicted in Figure 12 with the vertices of τB given in Figure 9.

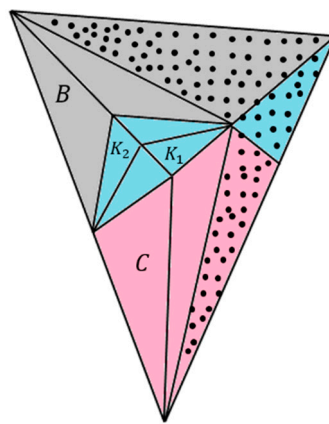


Figure 12. Top view of τA (bottom view is the same as bottom view of τB - dotted region).

The vertices of $C \{(0,0,0), \frac{1}{2}(\tau, 0, 1), \frac{1}{2}(\tau^2, 1, 0), \frac{1}{2}(\tau^2, \tau, 1)\}$ can be obtained from those in Figure 2 by a translation $\frac{1}{2}(-\tau, -\tau, -\tau)$ followed by a rotation

$$g_C = \frac{1}{2} \begin{bmatrix} -1 & \sigma & -\tau \\ \sigma & -\tau & 1 \\ -\tau & 1 & -\sigma \end{bmatrix} \quad (28)$$

Vertices of K_1 and K_2 are given by

$$\begin{aligned} K_1 &: \left\{ \frac{1}{2}(\tau, 0, 1), \frac{1}{2}(\tau^2, 1, 0), \frac{1}{2}(\tau^2, \tau, 1), \frac{1}{4}(3\tau + 1, \tau, 1) \right\}, \\ K_2 &: \left\{ \frac{1}{2}(\tau, 0, 1), \frac{1}{2}(\tau^2, \tau, 1), \frac{1}{4}(3\tau + 1, \tau, 1), \frac{1}{2}(2\tau, -\sigma, 1) \right\}. \end{aligned} \quad (29)$$

To obtain K_1 and K_2 with these vertices, first rotate K by g_{K_1} and g_{K_2} given by the matrices

$$g_{K_1} = \frac{1}{2} \begin{bmatrix} \sigma & \tau & -1 \\ \tau & 1 & -\sigma \\ 1 & \sigma & -\tau \end{bmatrix}, \quad g_{K_2} = \frac{1}{2} \begin{bmatrix} \sigma & \tau & 1 \\ \tau & 1 & \sigma \\ 1 & \sigma & \tau \end{bmatrix}, \quad (30)$$

and translate both by the vector $t_{K_1} = \frac{1}{2}(\tau, 0, 1)$. The vertices of B in Figure 12 can be obtained by a rotation then a translation given, respectively, by

$$g_B = \frac{1}{2} \begin{bmatrix} -\tau & -1 & \sigma \\ -1 & -\sigma & \tau \\ -\sigma & -\tau & 1 \end{bmatrix}, \quad t_B = \frac{1}{2}(\tau^3, 0, \tau^2). \quad (31)$$

All these procedures are described in Table 3, which shows the rotations and translations both in E_{\parallel} and D_6 spaces.

Table 3. Rotation and translation in H_3 and D_6 (see the text for the definition of rotations in $E_{||}$ space).

H_3		D_6
$\tau K=B+K$		
g_K	←rotation→	$(\bar{136})(24\bar{5})$
$t_K = \frac{\epsilon}{2}(\tau, \tau^2, 0)$	←translation→	$\frac{1}{2}[(m_1 + 5m_2)l_1 + (m_1 + m_2)(l_2 + l_3 + l_4 + l_5 - l_6)]$
$\tau B=C+4K+B_1+B_2$		
g_B	←rotation→	$(3)(126\bar{45})$
g_{4K}	←rotation→	$(1)(23)(45)(6)$
$t_{4K} = \frac{\epsilon}{2}(\tau, 0, 1)$	←translation→	$m_1l_5 + m_2(l_1 - l_2 + l_3 - l_4 - l_6)$
g_{B_1}	←rotation→	$(1643\bar{5})(2)$
g_{B_2}	←rotation→	$(152\bar{152}), (364\bar{364})$
$t_B = \frac{\epsilon}{2}(\tau^3, 0, \tau^2)$	←translation→	$\frac{1}{2}[(3m_1 + 5m_2)l_5 + (m_1 + 3m_2)(l_1 - l_2 + l_3 - l_4 - l_6)]$
$\tau C=K_1+K_2+C_1+C_2+A$		
g_{K_1}	←rotation→	$(5\bar{4621})(3)$
	(identity translation)	
g_{K_2}	←rotation→	$(1\bar{1})(634\bar{52634}\bar{52})$
$t_K = \frac{\epsilon}{2}(\tau^2, \tau, 1)$	←translation→	$(m_1 + m_2)(l_1 + l_5) + 2m_2(l_3 - l_6)$
$t_C = -\frac{\epsilon}{2}(\tau, \tau, \tau)$	←translation→	$-\frac{1}{2}[(m_1 + 3m_2)(l_1 + l_3 + l_5) + (m_1 - m_2)(l_2 - l_4 - l_6)]$
g_{C_1}	←rotation→	$(1)(4)(2\bar{6})(35)$
g_{C_2}	←rotation→	$(1)(35642)$
$t_C = \frac{\epsilon}{2}(\tau^2, \tau^2, \tau^2)$	←translation→	$(m_1 + 2m_2)(l_1 + l_3 + l_5) + m_2(l_2 - l_4 - l_6)$
g_A	←rotation→	$(1)(6)(23)(45)$
$t_A = \frac{\epsilon}{2}(\tau^2, 0, \tau)$	←translation→	$\frac{1}{2}[(m_1 + 5m_2)l_5 + (m_1 + m_2)(l_1 - l_2 + l_3 - l_4 - l_6)]$
$\tau A=C+K_1+K_2+B+\tau B$		
$t_C = -\frac{\epsilon}{2}(\tau, \tau, \tau)$	←translation→	$-\frac{1}{2}[(m_1 + 3m_2)(l_1 + l_3 + l_5) + (m_1 - m_2)(l_2 - l_4 - l_6)]$
g_C	←rotation→	$(1\bar{1})(2\bar{4})(36)(5\bar{5})$
g_{K_1}	←rotation→	$(1)(2543\bar{6})$
g_{K_2}	←rotation→	$(1)(4)(2\bar{6})(35)$
$t_K = \frac{\epsilon}{2}(\tau, 0, 1)$	←translation→	$m_1l_5 + m_2(l_1 - l_2 + l_3 - l_4 - l_6)$
g_B	←rotation→	$(65\bar{1651}), (423423)$
$t_B = \frac{\epsilon}{2}(\tau^3, 0, \tau^2)$	←translation→	$\frac{1}{2}[(3m_1 + 5m_2)l_5 + (m_1 + 3m_2)(l_1 - l_2 + l_3 - l_4 - l_6)]$

4. Discussions

The six-dimensional reducible representation of the icosahedral subgroup of the point group of D_6 is decomposed into the direct sum of its two three-dimensional representations described also by the direct sum of two graphs of icosahedral group. We have shown that the subset of the D_6 lattice characterized by a pair of integers (m_1, m_2) with $m_1 + m_2 = \text{even}$ projects onto the Platonic and Archimedean polyhedra possessing icosahedral symmetry, which are determined as the orbits of the fundamental weights v_i or their multiples by τ^n . The edge lengths of the Danzer tiles are related to the weights of the icosahedral group H_3 and via Table 1 to the weights of D_6 , a group theoretical property, which has not been discussed elsewhere. It turns out that the tetrahedron K constitutes the fundamental region of the icosahedral group H_3 as being the cell of the rhombic triacontahedron. Images of the Danzer tiles and their inflations are determined in D_6 by employing translations and icosahedral

rotations. This picture gives a one-to-one correspondence between the translations–rotations of 3D space and 6D space.

Faces of the Danzer tiles are all parallel to the faces of the rhombic triacontahedron; in other words, they are all orthogonal to the two-fold axes. Since the faces of the Ammann rhombohedral tiles are orthogonal to the two-fold axes of the icosahedral group it is this common feature that any tilings obtained from the Ammann tiles either with decoration or in the form of the Socolar–Steinhardt model can also be obtained by the Danzer tiles. These geometrical properties have not been studied from the group theoretical point of view, a subject which is beyond the present work but definitely deserves to be studied. Note that the inflation introduces a cyclic permutation among the rhombic triacontahedron, “B-polyhedron”, and “C-polyhedron”, as they occur alternatively centered at the origin.

Another novel feature of the paper is to show that *ABCK* tiles and their inflations are directly related to the transformations in the subset of D_6 lattice characterized by integers (m_1, m_2) , leading to an alternative projection technique different from the cut and project scheme. Details of the composition of the *ABCK* tiles into a structure with long-range quasiperiodic order follows from the inflation matrix (see for instance [4]).

Author Contributions: Conceptualization, M.K., N.O.K., A.A.-S.; methodology, M.K., A.A.-S., N.O.K.; software, A.A.-S., N.O.K.; validation, M.K., A.A.-S., N.O.K.; formal analysis, A.A.-S., N.O.K.; investigation, A.A.-S., M.K., N.O.K.; writing-original draft preparation, M.K., A.A.-S., N.O.K.; writing-review and editing, M.K., N.O.K., A.A.-S.; visualization, A.A.-S.; N.O.K.; project administration, M.K.; supervision, M.K., N.O.K., A.A.-S. All authors have read and agreed to the published version of the manuscript.

Funding: This research was partly funded by Sultan Qaboos University, Om an.

Acknowledgments: We would like to thank Ramazan Koc for his contributions to Figures 6 and 7.

Conflicts of Interest: The authors declare no conflict of interest.

References

1. Di Vincenzo, D.; Steinhardt, P.J. *Quasicrystals: The State of the Art*; World Scientific Publishers: Singapore, 1991.
2. Janot, C. *Quasicrystals: A Primer*; Oxford University Press: Oxford, UK, 1993.
3. Senechal, M. *Quasicrystals and Geometry*; Cambridge University Press: Cambridge, UK, 1995.
4. Baake, M.; Grimm, U. *Aperiodic Order; A Mathematical Invitation*; Cambridge University Press: Cambridge, UK, 2013; Volume 1.
5. Socolar, J.E.S.; Steinhardt, P.J. Quasicrystals. II. Unit-cell configurations. *Phys. Rev. B* **1986**, *34*, 617–647. [[CrossRef](#)] [[PubMed](#)]
6. Danzer, L.; Papadopolos, D.; Talis, A. Full equivalence between Socolar’s tilings and the (A, B, C, K)-tilings leading to a rather natural decoration. *J. Mod. Phys.* **1993**, *7*, 1379–1386. [[CrossRef](#)]
7. Roth, J. The equivalence of two face-centered icosahedral tilings with respect to local derivability. *J. Phys. A Math. Gen.* **1993**, *26*, 1455–1461. [[CrossRef](#)]
8. Danzer, L. Three-dimensional analogs of the planar Penrose tilings and quasicrystals. *Discrete Math.* **1989**, *76*, 1–7. [[CrossRef](#)]
9. Katz, A. *Some Local Properties of the Three-Dimensional Tilings, in Introduction of the Mathematics of Quasicrystals*; Jaric, M.V., Ed.; Academic Press, Inc.: New York, NY, USA, 1989; Volume 2, pp. 147–182.
10. Hann, C.T.; Socolar, J.E.S.; Steinhardt, P.J. Local growth of icosahedral quasicrystalline tilings. *Phys. Rev. B* **2016**, *94*, 014113. [[CrossRef](#)]
11. Available online: <https://www.math.uni-bielefeld.de/~frettlow/papers/ikosa.pdf> (accessed on 1 October 2020).
12. Kramer, P. Modelling of quasicrystals. *Phys. Scr.* **1993**, *1993*, 343–348. [[CrossRef](#)]
13. Koca, M.; Koca, N.; Koc, R. Group-theoretical analysis of aperiodic tilings from projections of higher-dimensional lattices *Bn. Acta Cryst. A* **2015**, *71*, 175–185. [[CrossRef](#)] [[PubMed](#)]
14. Kramer, P.; Andriele, M. Inflation and wavelets for the icosahedral Danzer tiling. *J. Phys. A Math. Gen.* **2004**, *37*, 3443–3457. [[CrossRef](#)]
15. Koca, M.; Koca, N.; Al-Siyabi, A.; Koc, R. Explicit construction of the Voronoi and Delaunay cells of W (An) and W (Dn) lattices and their facets. *Acta. Cryst. A* **2018**, *74*, 499–511. [[CrossRef](#)] [[PubMed](#)]

16. Conway, J.H.; Sloane, N.J.A. *Sphere Packings, Lattices and Groups*, 3rd ed.; Springer New York Inc.: New York, NY, USA, 1999.
17. Koca, M.; Koc, R.; Al-Barwani, M. on crystallographic Coxeter group H4 in E8. *J. Phys. A Math. Gen.* **2001**, *34*, 11201–11213. [[CrossRef](#)]
18. Alhevaz, A.; Baghipur, M.; Shang, Y. On generalized distance Gaussian Estrada index of graphs. *Symmetry* **2019**, *11*, 1276. [[CrossRef](#)]
19. Coxeter, H.S.M. *Regular Polytopes*, 3rd ed.; Dover Publications: Mineola, NY, USA, 1973.
20. Humphreys, J.E. *Reflection Groups and Coxeter Groups*; Cambridge University Press: Cambridge, UK, 1992.

Publisher’s Note: MDPI stays neutral with regard to jurisdictional claims in published maps and institutional affiliations.



© 2020 by the authors. Licensee MDPI, Basel, Switzerland. This article is an open access article distributed under the terms and conditions of the Creative Commons Attribution (CC BY) license (<http://creativecommons.org/licenses/by/4.0/>).